

***K*-emission spectra of Zn, ZnS, and ZnSe within dipole and quadrupole approximations**

R. Laihia

Graduate School of Materials Research, Department of Physics, University of Turku, FIN-20014 Turku, Finland

K. Kokko

Department of Physics, University of Turku, FIN-20014 Turku, Finland

W. Hergert

Department of Physics, Martin-Luther-University, Friedemann-Bach-Platz 6, D-06099 Halle, Germany

J. A. Leiro

Department of Applied Physics, University of Turku, FIN-20014 Turku, Finland

(Received 19 February 1998)

The present work deals with the x-ray $K\beta_{2,5}$ -emission bands and the electronic structures of Zn metal as well as ZnS and ZnSe compounds. The above-mentioned compounds were chosen the subject of the investigation because they are ideal materials to study the $3d$ - $4p$ hybridization since the Zn d band is about 10 eV below the Fermi level and therefore the $K\beta_2$ and $K\beta_5$ spectra are quite well separated from each other. The $K\beta_5$ spectra of ZnS and ZnSe compounds are found to be largely caused by the quadrupole radiation. The electronic structures of the investigated materials are obtained by using the linear muffin-tin orbital method. The calculations show that for cubic crystals the quadrupole spectra can have a strong polarization dependence although the dipole spectra are independent of polarization. The theoretical spectra of the investigated materials are treated in the framework of the full band-structure representation. [S0163-1829(98)06927-6]

I. INTRODUCTION

Zn compounds (ZnS, ZnSe) are well-known materials in science and technology. ZnS is an important raw material in mining industry for the production of Zn metal. ZnSe turns out to be a useful compound in semiconductor technology. Due to its wide band gap, ZnSe has been a promising material for the development of blue-light lasers.¹⁻³ For the development of new materials the knowledge of their electronic structure is most important. X-ray emission spectroscopy (XES) offers an ideal experimental tool for the investigation of semiconductors and insulators because of the absence of the charging effects. On the other hand, these experiments give detailed information concerning the electronic structure of valence electrons. Furthermore, XES measurements are site dependent as far as the different atomic types of the investigated compounds are concerned. This site dependence is caused by the creation of the localized core hole of a specific atom by an x-ray photon. One of the first x-ray investigations of the K -emission bands of ZnSe is due to Drahoukoupil and Šimůnek.⁴ For recent investigations dealing with the ZnS and ZnSe compounds we pay attention to Refs. 5-10.

In order to interpret experimental x-ray emission bands theoretical investigations are needed. The local-partial density of states (DOS) gives information concerning site dependent electronic states. In the linear muffin-tin orbital (LMTO) (Ref. 11) band-structure calculation method the local-partial DOS is obtained in a natural way. Considering the interaction of electromagnetic radiation with matter the obtained energy spectrum of the radiation is of special im-

portance. In the energy range of γ radiation one could expect a quite large quadrupole contribution to the spectrum, but in the case of x radiation the quadrupole contribution is usually omitted. However, for hard x rays the quadrupole spectrum may give an important contribution. The quadrupole contribution is definitely measurable as Fabian *et al.*¹² have shown for metallic selenium. For metallic gallium a similar feature has also been observed.¹³ A Zn atom in a solid provides an ideal case to study the K -emission spectra in dipole and quadrupole approximations. This is because the Zn $3d$ band is concentrated at the bottom of the s - p valence band. Due to this property, the $3d$ band can be clearly separated from the main s - p valence band, but at the same time it is energetically not too far from the valence band so that a considerable interaction between the $3d$ and s - p valence electrons is expected. The dipole spectrum of pure Zn has been calculated earlier.¹⁴ In the present work, we discuss the Zn K -emission spectra of Zn, ZnS, and ZnSe in terms of the dipole and quadrupole approximations and use the obtained theoretical spectra to analyze the experimental $K\beta_{2,5}$ spectra of the investigated materials.

II. THEORY

A. Spectra in dipole and quadrupole approximations

For valence-band x-ray emission the intensity of the radiation is determined by the density of states of the valence electrons and by the matrix element $\langle f | \exp(-i\mathbf{k} \cdot \mathbf{r}) \hat{\mathbf{e}} \cdot \mathbf{p} | i \rangle$,¹⁵ where $\langle f |$ and $| i \rangle$ refer to the final and initial states of the electronic system, which we assume to be nonmagnetic, \mathbf{k}

and \mathbf{r} are the wave vector of the emitted x radiation and the position vector in real space, respectively, $\hat{\mathbf{e}}$ is the polarization vector of the radiation and \mathbf{p} is the momentum operator of the electron. Expanding the exponential function in terms of the power series $\exp(-i\mathbf{k}\cdot\mathbf{r})=1-i\mathbf{k}\cdot\mathbf{r}-(\mathbf{k}\cdot\mathbf{r})^2/2+\dots$ leads to the series representation of the matrix element. In this series the first term leads to the dipole term. The electric part of the second term containing $i\mathbf{k}\cdot\mathbf{r}$ leads to the quadrupole term. The dipole term gives a nonzero contribution if the angular momentum quantum numbers (l) of the $\langle f|$ and $|i\rangle$ states differ by one ($\Delta l = \pm 1$, dipole selection rule). The quadrupole term gives a nonzero contribution if $\Delta l = \pm 2$. For soft x rays (small $|\mathbf{k}|$) the quadrupole and higher terms are small compared to the dipole term, which gives the leading contribution to the observed spectrum. Thus, the relative intensities of the dipole and quadrupole spectra depend on the absolute value of the wave vector \mathbf{k} of the emitted x radiation.

According to Fermi's golden rule we can obtain the intensity of the dipole and quadrupole radiation from the following expression:¹⁶

$$W_{fi} = \frac{\omega e^2}{hm^2c^3} |\langle f | \exp(-i\mathbf{k}\cdot\mathbf{r}) \hat{\mathbf{e}} \cdot \mathbf{p} | i \rangle|^2 \delta(E_f - E_i + \hbar\omega), \quad (1)$$

where ω is the angular frequency of the radiation and m is the mass of the electron. E_i and E_f are the energy eigenvalues of the initial and final states, respectively. To calculate the emission spectrum of a solid one has to consider the transition from the valence states to the corresponding core state. Therefore, one gets for the dipole and quadrupole radiation¹⁵

$$I_D(E, \hat{\mathbf{e}}) = CE^3 \sum_{\mathbf{kb}}^{occ.} \sum_c |\langle \Phi_c | r(\hat{\mathbf{e}} \cdot \hat{\mathbf{r}}) | \Psi_{\mathbf{kb}} \rangle|^2 \times \delta(E_c - E_{\mathbf{kb}} + E), \quad (2)$$

$$I_Q(E, \hat{\mathbf{e}}, \hat{\mathbf{k}}) = \frac{\pi^2}{h^2c^2} CE^5 \sum_{\mathbf{kb}}^{occ.} \sum_c |\langle \Phi_c | r^2(\hat{\mathbf{e}} \cdot \hat{\mathbf{r}})(\hat{\mathbf{k}} \cdot \hat{\mathbf{r}}) | \Psi_{\mathbf{kb}} \rangle|^2 \times \delta(E_c - E_{\mathbf{kb}} + E).$$

The constant C is given by $C = 8\pi^3 e^2 / (h^4 c^3)$ and $\mathbf{r} = r\hat{\mathbf{r}}$. $E_{\mathbf{kb}}$ and E_c are the energy eigenvalues of the valence and core states, respectively, $E = \hbar\omega$ is the energy of the emitted radiation, and b is the band index. The first sum is over the occupied valence states and the second sum is over the relevant core states. The explicit forms of the electronic states Φ_c and $\Psi_{\mathbf{kb}}$ and the matrix elements are shown in the Appendix. Since we are interested only in the relative magnitudes of the dipole and quadrupole spectra the common numerical factor C was left out from the above spectra in our calculations. The tensor operator formalism was used to calculate the dipole and quadrupole matrix elements.¹⁷

B. Symmetry considerations

The polarization vector $\hat{\mathbf{e}}$ and the direction of the wave vector $\hat{\mathbf{k}}$ of the emitted radiation can be expressed in spherical coordinates as

$$\hat{\mathbf{e}} = (\sin \theta \cos \phi, \sin \theta \sin \phi, \cos \theta), \quad (3)$$

$$\hat{\mathbf{k}} = (\cos \theta \cos \phi \cos \psi - \sin \phi \sin \psi, \cos \theta \sin \phi \cos \psi + \cos \phi \sin \psi, -\sin \theta \cos \psi),$$

where the angle ψ specifies the direction of $\hat{\mathbf{k}}$ in the plane perpendicular to $\hat{\mathbf{e}}$. Using the spherical tensors representation (cf. Ref. 22) we get for the cubic symmetry

$$I_D(E, \hat{\mathbf{e}}) = I_D^{(0,0)}(E), \quad (4)$$

$$I_Q(E, \hat{\mathbf{e}}, \hat{\mathbf{k}}) = I_Q^{(0,0)}(E) + \frac{1}{\sqrt{14}} [35 \sin^2 \theta \cos^2 \theta \cos^2 \psi + 5 \sin^2 \theta \sin^2 \psi - 4 + 5 \sin^2 \theta (\cos^2 \theta \cos^2 \psi \cos 4\phi - \sin^2 \psi \cos 4\phi - 2 \cos \theta \sin \psi \cos \psi \sin 4\phi)] I_Q^{(4,0)}(E)$$

and for the hexagonal symmetry

$$I_D(E, \hat{\mathbf{e}}) = I_D^{(0,0)}(E) - \frac{1}{\sqrt{2}} (3 \cos^2 \theta - 1) I_D^{(2,0)}(E), \quad (5)$$

$$I_Q(E, \hat{\mathbf{e}}, \hat{\mathbf{k}}) = I_Q^{(0,0)}(E) + \sqrt{\frac{5}{14}} \times (3 \sin^2 \theta \sin^2 \psi - 1) I_Q^{(2,0)}(E) + \frac{1}{\sqrt{14}} (35 \sin^2 \theta \cos^2 \theta \cos^2 \psi + 5 \sin^2 \theta \sin^2 \psi - 4) I_Q^{(4,0)}(E).$$

According to Eqs. (4) and (5) the dipole intensity has no angle dependence in the case of the cubic symmetry. However, in hexagonal crystals the intensity of the dipole transition depends on the angle of the polarization vector to the c axis of the crystal. Two measurements with the polarization vector parallel and perpendicular to the c axis allow us to determine the σ and π components of the dipole spectrum in hexagonal crystals [$I_\sigma(E) = I_D^{(0,0)}(E) + I_D^{(2,0)}(E)/\sqrt{2}$, $I_\pi(E) = I_D^{(0,0)}(E) - \sqrt{2} I_D^{(2,0)}(E)$]. The angular dependence of the quadrupole radiation given in Eqs. (4) and (5) can be used to find the optimum experimental conditions producing the maximum and minimum values of the quadrupole intensity. The unpolarized (isotropic) spectra are obtained by averaging over the directions of the polarization and wave vectors.

$$\bar{I}_D(E) = \frac{1}{4\pi} \int I_D(E, \hat{\mathbf{e}}) \sin \theta d\theta d\phi,$$

$$\bar{I}_Q(E) = \frac{1}{8\pi^2} \int I_Q(E, \hat{\epsilon}, \hat{\mathbf{k}}) \sin \theta \, d\theta \, d\phi \, d\psi, \quad (6)$$

which leads for the cubic and hexagonal symmetry to

$$\bar{I}_D(E) = I_D^{(0,0)}(E), \quad (7)$$

$$\bar{I}_Q(E) = I_Q^{(0,0)}(E).$$

III. RESULTS AND DISCUSSION

In the following we discuss the experimental x-ray K -emission spectra in the framework of the dipole and quadrupole approximations. Quite often the dipole spectrum depends on the polarization and the quadrupole spectrum depends on both the direction and polarization of the emitted radiation. The dipole selection rule is assumed to be approximately valid in XES, which allows one to investigate the electronic structure of materials by using XES data and the partial DOS and transition matrix elements. In high-energy x-ray spectroscopic studies some quadrupole lines may be found since the dipole selection rule may be only approximately valid. This could happen, e.g., in analyzing the emission spectra of heavy elements. The intensity of the quadrupole line ($1s^{-1} \rightarrow 3d^{-1}$, a hole moves from the $1s$ to the $3d$ states) should be lower than that of the corresponding dipole line ($1s^{-1} \rightarrow 4p^{-1}$). Due to this property it has been difficult to measure the quadrupole contribution and correspondingly in theoretical considerations the quadrupole part has been usually discarded. This has led to the debate of the origin of the peaks of the K -emission spectra observed at energies where both p and d valence states coexist. The availability of first-principles theoretical emission spectra may help to design and interpret XES experiments, which can be used to separate experimental spectra into dipole and quadrupole components. Usually, the $K\beta_5$ spectrum is associated with the quadrupole selection rule and the $K\beta_2$ spectrum with the dipole selection rule (Fig. 2 in Ref. 18). The experimental K -emission band possesses the lifetime broadening of the $1s$ level, which has been calculated to be about 1.67 eV.¹⁹ In addition, the effect of the instrumental broadening is of the same order of magnitude. Therefore, the experimental spectra are smoother than the theoretical ones.

Analyzing experimental x-ray emission spectra by comparing them with the calculated l -resolved electronic DOS has been quite successful in increasing the understanding of the electronic structure of materials and the relation between the electronic structure and the chemical composition of materials. Very often the positions and intensities of experimental emission peaks can be identified with the corresponding quantities in the calculated DOS curve. However, in many cases one needs a more accurate theoretical description than the DOS curves can give. For instance, the question whether the peak in the K -emission spectra of Zn and its compounds at the binding energy of 6–9 eV ($K\beta_5$) is due to the quadrupole or dipole radiation has been under discussion for a long time, but no definite answer has been obtained so far. In the following we hope to shed more light on this matter by combining the first-principles electronic structure calculations with the full treatment of the transition probability in

the x-ray emission process. We analyze the experimental valence-band Zn K -emission spectra of pure Zn as well as the ZnS and ZnSe compounds by considering the theoretical emission spectrum in both the dipole and quadrupole approximations [Eq. (2)].

A. Unpolarized spectra

In our earlier work¹⁸ we came to the conclusion that the $K\beta_5$ spectrum of Zn and the Zn compounds is probably associated to a considerable extent with the quadrupole transition. The analysis in our earlier work is, however, based only on the electronic DOS being in that sense incomplete. In the following we will reanalyze our experimental data in a more quantitative level by using theoretical first-principles dipole and quadrupole spectra. This approach allows a direct interpretation of the experimental $K\beta_5$ spectra.

Our measurements were made for polycrystalline samples. These kind of samples consist of microcrystals with random orientations and therefore the measured spectra are unpolarized. Thus the theoretical spectra have to be averaged [Eq. (7)] over the polarization and direction of the radiation before comparing them with the experimental spectra. Considering the experimental x-ray K -emission valence-band spectrum of pure Zn (Ref. 18) one observes two distinct peaks; the major peak is just below the Fermi energy and the minor peak is at about 9 eV below the Fermi energy. It has been shown that the major peak ($K\beta_2$) can be related to the p -DOS of pure Zn metal,¹⁸ but in the case of the minor peak ($K\beta_5$) it is not clear to what extent the peak intensity should be related to the p -DOS (hybridization of the $4p$ states with the $3d$ states—dipole radiation) or to the d -DOS (quadrupole radiation).

In Fig. 1 the calculated unpolarized Zn dipole and quadrupole K -emission spectra of Zn, ZnS, and ZnSe are shown. Since we are mainly interested in the $K\beta_5$ spectrum, we concentrate on the energy region of the Zn $3d$ band. Within this energy region the theoretical spectrum consists mainly of the dipole part in pure Zn, but in ZnS and ZnSe the quadrupole and dipole contributions to the total spectrum are of the same order of magnitude. The intensity of the dipole spectrum in the $K\beta_5$ energy region decreases considerably when going from pure Zn to ZnS and ZnSe, whereas the intensity of the quadrupole spectrum does not change so much. In the following we compare the integrated $K\beta_5$ intensities of ZnS and ZnSe with those of pure Zn. As Fig. 2 shows, the dipole part of $K\beta_5$ in ZnS is only 17% of that in pure Zn. In ZnSe the corresponding ratio is 22%. For the quadrupole part of $K\beta_5$ these ratios are 50% and 78% for ZnS and ZnSe, respectively. Figure 2 also reveals the importance of the matrix elements in the calculation of the spectra. If the matrix element is omitted, the obtained intensity ratios will be considerably higher than those calculated by using the matrix elements. This increase varies from about 200% for the dipole transition in ZnS to about 25% for the quadrupole transition in ZnSe. The general trend is that in the dipole transitions the effect of the matrix element is more important than in the quadrupole transitions and for ZnS it is more pronounced than for ZnSe as far as the spectral quantities of ZnS and ZnSe are compared to those of pure Zn.

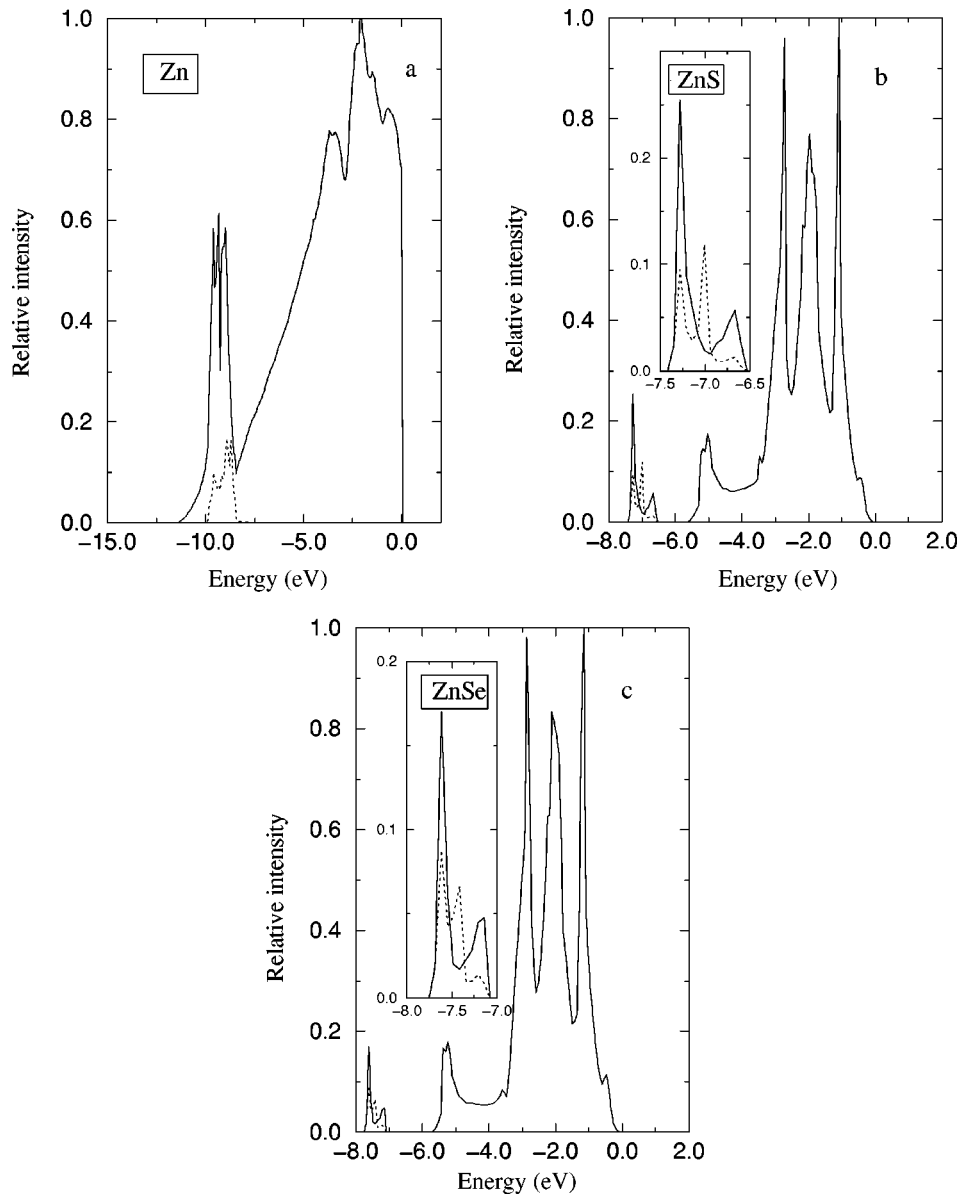


FIG. 1. The theoretical unpolarized dipole (solid line) and quadrupole (dashed line) x-ray K -emission spectra of Zn (a), ZnS (b), and ZnSe (c). The top of the occupied part of the band is at 0 eV and the spectra are renormalized to one at the highest peak.

The total intensity of the calculated minor spectral peak at higher binding energies (dipole + quadrupole) compared to the intensity of the major peak at lower binding energies is 12% for pure Zn, 6% for ZnS, and 4% for ZnSe. This can be compared with the ratios estimated from the experimental spectra, which are 10%, 7%, and 8% for pure Zn, ZnS, and ZnSe, respectively. The discrepancy in the case of ZnSe can be related to the large $K\beta_2$ intensity. Although the absolute intensity of the theoretical $K\beta_5$ spectrum of ZnSe is larger than that of ZnS the ratio $K\beta_5/K\beta_2$ is smaller for ZnSe than for ZnS. This suggests that the theoretical charge transfer to Zn 4*p*-like states would be too large for ZnSe. If the quadrupole transitions were not included in the theoretical spectra the overall agreement with the experiments would be worse since the quadrupole contribution is about 40% of the whole $K\beta_5$ spectrum of ZnS and ZnSe. However, because conventional band-structure calculation methods may overestimate the 3*d*-4*p* intraband hybridization,²⁰ which is especially im-

portant for pure Zn, it would be useful to investigate the dipole and quadrupole intensities by using other theoretical methods as well.

B. Polarized spectra

As shown in Sec. II, for anisotropic single crystals the dipole contribution of the emission spectrum depends on the polarization (the quadrupole contribution also on the direction) of the emitted radiation. Thus, it may be possible to resolve the emission spectrum into the dipole and quadrupole parts by considering the angular dependence of the spectrum. The dipole and quadrupole transitions in K -emission spectra are associated with *p* and *d* valence states, respectively. Because the spatial distributions of the *p* and *d* valence states around an atom are usually quite different from each other, resolving the dipole and quadrupole contributions in experimental spectra may give a new insight of the physical prop-

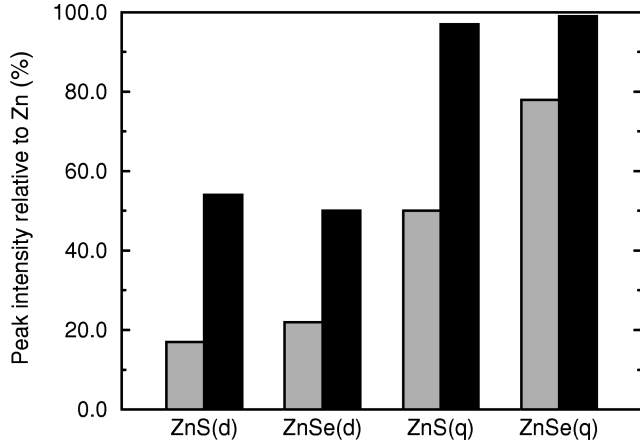


FIG. 2. The relative intensity of the $K\beta_5$ peak of ZnS and ZnSe, compared to pure Zn, in the dipole (d) and quadrupole (q) approximations. The black bars show the situation without the matrix elements (DOS data).

erties of the investigated materials. Effects, e.g., due to the change in volume, crystal distortion, and composition could be investigated by this method.

The polarized K -emission spectra of hcp Zn have been measured by Dräger and Brümmer (Ref. 21, and references therein). The shape and the intensity ratio of the experimental $K\beta_2\pi$ and $K\beta_2\sigma$ spectra can be reproduced quite well by using Shaw's pseudopotential method.¹⁴ For hcp metals the peak intensity ratio Q of the maxima of the experimental I_π and I_σ spectra depends on the ratio of the lattice parameters (c/a) as follows: $Q \leq 1$ if $c/a \geq 1.633$.²¹ Our theoretical dipole spectra contain the hybridization peak due to the Zn $3d$ states lying at about 9 eV below the Fermi energy [Fig. 3(a)]. This peak is missing in the theoretical dipole spectra of Renert *et al.*¹⁴ because they did not have the Zn $3d$ states in their basis set. The overall shapes of our π and σ spectra are rather similar except in the energy region of 0–5 eV below the Fermi energy, where I_σ is considerably more intense than I_π . Good agreement with the experiment²¹ is obtained as far as the intensity ratio Q is concerned. It is also interesting to note that in I_σ the $3d$ - $4p$ hybridization occurs in a wider energy range than in I_π .

The Zn quadrupole spectra [$\hat{\epsilon} \parallel (1,0,0)$ and $\hat{\mathbf{k}}$ in yz plane] are shown in Fig. 3(b). The quadrupole peak is highest when $\hat{\mathbf{k}}$ is parallel to the z axis. The peak gets gradually lower and broader when the $\hat{\mathbf{k}}$ vector is rotated in the yz plane from the z -axis alignment to the y -axis alignment. Our calculations suggest that using a high resolution technique it may be possible to detect the quadrupole contribution in the experimental $K\beta_5$ spectrum by fixing the polarization and rotating the direction of the radiation.

In Figs. 3(c) and 3(d) the quadrupole spectra of ZnS and ZnSe are shown. The calculated cases [$\hat{\mathbf{k}} \parallel (1,1,0)$ and $\hat{\epsilon} \parallel (0,0,1)$ and $(1, -1, 0)$] are such that one expects largest possible differences between the obtained spectra.²² Because the relative intensity of the quadrupole part compared to the dipole part in $K\beta_5$ is larger in ZnS and ZnSe compounds than

in pure Zn, the quadrupole contribution in the experimental spectrum is expected to be easier to detect for ZnS and ZnSe than for pure Zn.

IV. CONCLUSIONS

For the quantitative comparison of the theoretical and experimental valence-band x-ray K -emission spectra of the investigated materials it is necessary to include both the dipole and quadrupole contributions in the considerations. X-ray emission measurements for these materials using single crystal samples would be highly valuable because by measuring the emitted radiation as a function of the direction of the radiation one can experimentally distinguish between the dipole and the quadrupole spectra. By comparing the experimental and theoretical spectra one could also draw conclusions about the feasibility of the one-particle local-density-approximation picture for the description of the valence electrons of transition metals with the interaction of electromagnetic radiation. Besides analyzing the experimental spectra the first-principles theoretical emission spectra can be used to design new XES experiments in an optimal way. Our calculations suggest that for pure Zn the $K\beta_5$ spectrum is mainly due to the dipole transitions, but for ZnS and ZnSe the quadrupole contribution is substantial too.

ACKNOWLEDGMENTS

Discussions with E. Ojala are gratefully acknowledged. The financial support of the Academy of Finland, Grant No. 34942 (R.L., J.A.L., and K.K.) and the Turku University Foundation (K.K.) is acknowledged.

APPENDIX: CALCULATIONAL PROCEDURE

The energy band structure and wave functions of the valence electrons and the corresponding core wave function needed in Eq. (2) were calculated using first-principles methods. For the valence wave functions we used LMTO-type functions

$$\Psi_{kb}(\mathbf{r}) = \sum_{\mathbf{q}L} i^l [A_{\mathbf{q}L}^{kb} \phi_{\nu\mathbf{q}l}(|\mathbf{r}-\mathbf{q}|) + B_{\mathbf{q}L}^{kb} \dot{\phi}_{\nu\mathbf{q}l}(|\mathbf{r}-\mathbf{q}|)] |l, m, m_s\rangle, \quad (\text{A1})$$

where \mathbf{q} is the position vector of an atom in the unit cell and $L = (l, m)$ and m_s are the orbital angular momentum, magnetic, and spin quantum numbers, respectively, b is the band index and \mathbf{k} is the wave vector of the electron. ν refers to the LMTO reference energy E_ν . $A_{\mathbf{q}L}^{kb}$ and $B_{\mathbf{q}L}^{kb}$ are coefficients, which depend on the crystal structure and potential of the investigated system. $\phi_{\nu\mathbf{q}l}(r)$ and $\dot{\phi}_{\nu\mathbf{q}l}(r)$ are the radial wave function and its energy derivative. The core state $\Phi_c(\mathbf{r})$ is localized in the region of a specific atom and can be approximated by an atomiclike state

$$\Phi_c(\mathbf{r}) = R_{qn}^c(r) |j, l, m_j\rangle. \quad (\text{A2})$$

The radial wave function depends on the atomic type at the site \mathbf{q} , n is the principal quantum number, j is the total angular-momentum quantum number, and m_j is the corre-

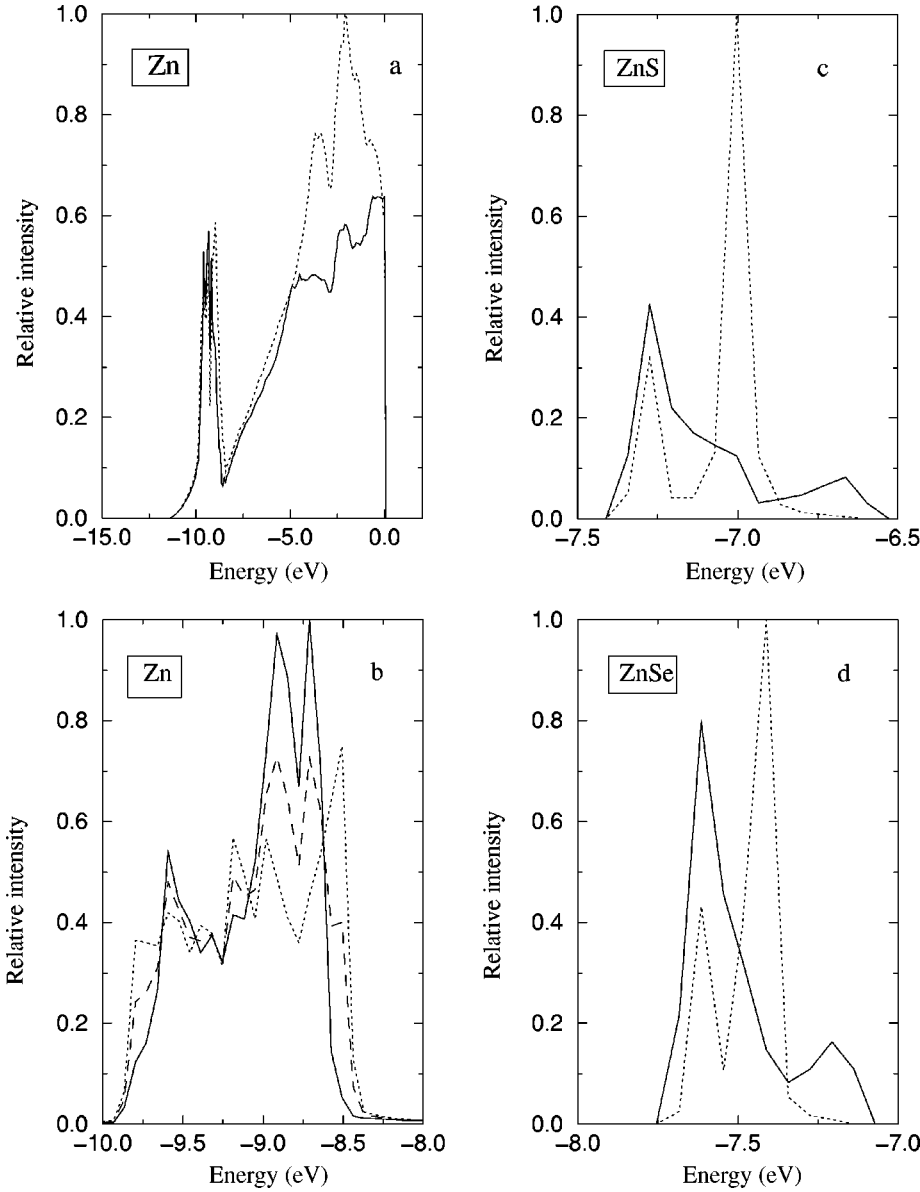


FIG. 3. The theoretical dipole and quadrupole x-ray K -emission spectra of Zn, ZnS, and ZnSe in the energy region of the Zn d band. (a) Dipole spectra of Zn; solid line, I_{π} ; dashed line, I_{σ} . (b) Quadrupole spectra of Zn, $\hat{\epsilon} = (1,0,0)$; solid line, $\hat{\mathbf{k}} = (0,0,1)$; dashed line, $\hat{\mathbf{k}} = (1/2)^{1/2}(0,1,1)$; and dotted line $\hat{\mathbf{k}} = (0,1,0)$. (c) and (d) Quadrupole spectra of ZnS and ZnSe, $\hat{\mathbf{k}} = (1/2)^{1/2}(1,1,0)$; solid line, $\hat{\epsilon} = (0,0,1)$; and dashed line, $\hat{\epsilon} = (1/2)^{1/2}(1, -1, 0)$.

sponding magnetic quantum number. Finally the dipole and quadrupole matrix elements have the following form:

$$\sum_{qL'} i^{l'} (A_{qL'}^{kb} M_{qnl, vl'}^r + B_{qL'}^{kb} \dot{M}_{qnl, vl'}^r) \times M_{jlm_j, l'm'_m_s}^a \delta_{\mathbf{q}, \mathbf{q}_e}, \quad (\text{A3})$$

where

$$M_{qnl, vl'}^r = \int R_{qnl}^c(r) \hat{O}^r(r) \phi_{vq l'}(r) r^2 dr, \quad (\text{A4})$$

$$\dot{M}_{qnl, vl'}^r = \int R_{qnl}^c(r) \dot{\hat{O}}^r(r) \phi_{vq l'}(r) r^2 dr, \quad (\text{A5})$$

$$M_{jlm_j, l'm'_m_s}^a = \langle j, l, m_j | \hat{O}^a(\hat{\mathbf{k}}) | l', m', m_s \rangle, \quad (\text{A6})$$

and where we have assumed that the atom with the core hole is located at $(\mathbf{q} = \mathbf{q}_e)$. In the dipole and quadrupole transitions the radial and angular operators are, respectively,

$$\hat{O}^r(r) = r, \quad \hat{O}^a(\hat{\mathbf{r}}) = \hat{\epsilon} \cdot \hat{\mathbf{r}}, \quad (\text{A7})$$

$$\hat{O}^r(r) = r^2, \quad \hat{O}^a(\hat{\mathbf{r}}) = (\hat{\epsilon} \cdot \hat{\mathbf{r}})(\hat{\mathbf{k}} \cdot \hat{\mathbf{r}}). \quad (\text{A8})$$

The electronic energy bands and wave functions needed for the spectrum calculations were obtained by using the scalar-relativistic LMTO method including the combined correction terms and the atomic-sphere approximation. The lattice parameters used in the calculations are $a = b = 2.66 \text{ \AA}$, $c = 4.95 \text{ \AA}$ for pure Zn, and $a = 5.41 \text{ \AA}$ and $a = 5.67 \text{ \AA}$ for the ZnS and ZnSe compounds, respectively. The crystal structures of pure Zn and the compounds are the hexagonal (hcp) and cubic zinc blende (ZnS), respectively. However, since ZnS and ZnSe possess a relatively open crystal structure we have to introduce empty spheres in the unit cell to obtain a good convergence in the calculations. The number of \mathbf{k} points in the irreducible wedge of the Brillouin zone was 112 for pure Zn and 55 for ZnS and ZnSe. For the details of the band-structure calculations we refer to our earlier study¹⁸ where the experimental x-ray K -emission spectra have been analyzed using the calculated DOS.

- ¹M. A. Haase, J. Qiu, J. M. DePuydt, and H. Cheng, *Appl. Phys. Lett.* **59**, 1272 (1991).
- ²J. M. Gaines, R. R. Drenten, K. W. Haberern, T. Marshall, P. Mensz, and J. Petruzzello, *Appl. Phys. Lett.* **62**, 2462 (1993).
- ³Z. Yu, J. Ren, Y. Lansari, B. Sneed, K. A. Bowers, C. Boney, D. B. Eason, R. P. Vaudo, K. J. Gossett, J. W. Cook, Jr., and J. F. Schetzina, *Jpn. J. Appl. Phys., Part 1* **32**, 663 (1993).
- ⁴J. Drahokoupil and A. Šimůnek, *J. Phys. C* **7**, 610 (1974).
- ⁵G. D. Lee, M. H. Lee, and J. Ihm, *Phys. Rev. B* **52**, 1459 (1995).
- ⁶A. Qteish, R. Said, N. Meskini, and A. Nazzal, *Phys. Rev. B* **52**, 1830 (1995).
- ⁷R. Markowski, M. Piacentini, D. Debowska, M. Zimnal-Starnawska, F. Lama, N. Zema, and A. Kisiel, *J. Phys.: Condens. Matter* **6**, 3207 (1994).
- ⁸Bal K. Agrawal, P. S. Yadav, and S. Agrawal, *Phys. Rev. B* **50**, 14 881 (1994).
- ⁹O. Zakharov, A. Rubio, X. Blase, M. L. Cohen, and S. G. Louie, *Phys. Rev. B* **50**, 10 780 (1994).
- ¹⁰H. C. Poon, Z. C. Feng, Y. P. Feng, and M. F. Li, *J. Phys.: Condens. Matter* **7**, 2783 (1995).
- ¹¹H. L. Skriver, in *The LMTO Method*, edited by M. Cardona and P. Fulde, Springer Series in Solid-State Sciences Vol. 41 (Springer, Berlin, 1984).
- ¹²D. J. Fabian, L. M. Watson, and C. A. W. Marshall, *Rep. Prog. Phys.* **34**, 657 (1971).
- ¹³J. A. Leiro, *X-Ray Spectrom.* **16**, 177 (1987).
- ¹⁴P. Rennert, H. Schelle, and U.-H. Gläser, *Phys. Status Solidi B* **121**, 673 (1984).
- ¹⁵A. B. Migdal, *Qualitative Methods in Quantum Theory* (Benjamin, MA, 1977), pp. 64 and 65.
- ¹⁶R. H. Landau, *Quantum Mechanics II* (Wiley, New York, 1990).
- ¹⁷L. C. Biedenharn and H. van Dam, *Quantum Theory of Angular Momentum* (Academic Press, New York, 1965).
- ¹⁸R. Laihia, J. A. Leiro, K. Kokko, and K. Mansikka, *J. Phys.: Condens. Matter* **8**, 6791 (1996).
- ¹⁹M. O. Krause and J. H. Oliver, *J. Phys. Chem. Ref. Data* **8**, 329 (1979).
- ²⁰D. L. Novikov, A. J. Freeman, N. E. Christensen, A. Svane, and C. O. Rodriguez, *Phys. Rev. B* **56**, 7206 (1997).
- ²¹G. Dräger and O. Brümmer, *Phys. Status Solidi B* **124**, 11 (1984).
- ²²C. Brouder, *J. Phys.: Condens. Matter* **2**, 701 (1990).